Calorimetric Study of Dynamical Heterogeneity in Toluene Solutions of Polystyrene

Nobuyuki Taniguchi,† Osamu Urakawa, and Keiichiro Adachi*

Department of Macromolecular Science, Graduate School of Science, Osaka University, Toyonaka, Osaka 560-0043, Japan

Received June 18, 2004; Revised Manuscript Received August 2, 2004

ABSTRACT: In an effort to clarify the effect of dynamical heterogeneity on the glass transition in binary systems, we measured the heat capacity C_p on concentrated toluene solutions of polystyrene (PS) using an adiabatic calorimeter. We also carried out dielectric measurements on the same system. Results indicate that the C_p vs temperature T curve of the solvent toluene/xylene(90/10) exhibits a sharp stepwise increase of C_p at the glass transition temperature T_g (= 115 K). In contrast, the C_p curves of PS/toluene solutions exhibit a double-sigmoidal shape. The configurational heat capacity ΔC_p around T_g has been determined by subtracting the heat capacity due to the lattice vibrations and intramolecular vibrations. We have further resolved ΔC_p into two sigmoidal curves using an empirical function. The T_gs corresponding to the two sigmoids are denoted as T_{g1} and T_{g2} ($T_{g1} > T_{g2}$). Two dielectric loss peaks termed α and β are assigned to segmental motions of PS and rotation of the toluene molecules, respectively. The dielectric glass transition temperatures T_α and T_β are defined as the temperatures at which the dielectric relaxation times for the α and β processes become 10^3 s, respectively. T_α and T_β agree well with the calorimetric T_{g1} and T_{g2}, respectively.

Introduction

Dynamical heterogeneity in miscible polymer blends has been actively investigated in the past decade with a wide variety of experimental techniques such as dielectric relaxation spectroscopy,[1−9] mechanical spectroscopy,[10−13] neutron scattering,[5] and NMR.[14−16] Dielectric and mechanical data indicate generally that miscible blends exhibit broader relaxation spectra than those of the components due to concentration fluctuation[17,18] and effects of self-concentration.[19] It is widely believed that segmental motions occur cooperatively, and hence miscible blends exhibit a broad unimodal α relaxation since the neighboring segments of the both components move together. However, when the difference of T_g between the components is large, cooperative motions are decoupled resulting in bimodal relaxation spectra.[2−5,10] Tomlin and Roland[20] found that polyisoprene (PI) and poly(vinyl ethylene) (PVE) are perfectly miscible. Colmenerro and co-workers[3,4] studied the dielectric behavior of PI/PVE blends and found a bimodal relaxation spectrum for the segmental mode process. Similar behavior was also reported for polystyrene (PS)/poly(vinyl methyl ether) (PVME).[10,14,15]

Decoupling of cooperative motions is well-known for polymer/diluent systems[21−29] in which dielectric loss peak due to the segmental motions (α) of the polymer and rotation of the diluent molecules (β) are observed in distinct frequency/temperature ranges due to dynamical heterogeneity. It is noted that the β process in polymer/diluent systems is due to the primary process (glass transition process) of diluents and not due to the secondary relaxation in the glassy state. Yada et al.[26] and Nakazawa et al.[27] reported that the dielectric loss curves for the α process of concentrated solutions of poly(vinyl acetate) (PVAc) are much broader than those of the components due to concentration fluctuation. Yoshizaki et al.[28] demonstrated for solutions of PS in alkylbenzenes that the broadening of the dielectric loss curves depends on the solvent quality. Recently, Hori et al.[29] reported the dielectric behavior of PS solutions in cyanopentylbipheny (5CB) having 3 times larger size than toluene and found that the extent of decoupling is small, and the loss peaks due to the both components merge with increasing temperature. Those experimental facts indicate that dynamical heterogeneity arises from two different origins: one is decoupling of cooperativity, or in other words the difference in the intrinsic mobilities of the components, and the other is heterogeneity in local composition. The former depends on the relative molecular size and intermolecular interactions of the components as found by Zhang et al.[8,9] for systems with specific interactions such as hydrogen bonding.

Long ago, Kauzmann[30] found that T_g of alcohols such as glycerol corresponds to the temperature at which the dielectric relaxation time τ becomes 100−1000 s, which is the time scale needed for measurements of the specific volume or heat capacity. If this hypothesis is applicable to a binary system in which motions of the components are decoupled, we expect that the system exhibits two T_gs corresponding to the different frozen-in temperatures of the components. So far, measurements of glass transition of binary systems have been mostly performed with thermal analyses (DSC). It is believed that a miscible system exhibits broad single T_g on the DSC diagram, and this has been used long as a criterion of miscibility. However, double glass transition phenomena were observed for various polymer/diluent systems by using DSC.[24,31−33] Those results originate in dynamical heterogeneity of polymer/diluent systems, and more careful calorimetric measurements are needed for understanding of the phenomena of dynamical heterogeneity since there is a limitation of the DSC method in the sensitivity. In this work we studied the glass transition in concentrated solutions of PS/toluene by measure-

† Present address: Toyobo Research Center Co. Ltd., 1-1 Katata-2, Otsu, 520-0292 Japan.
* Corresponding author.

10.1021/ma048788j CCC: $27.50
Published on Web 09/10/2004

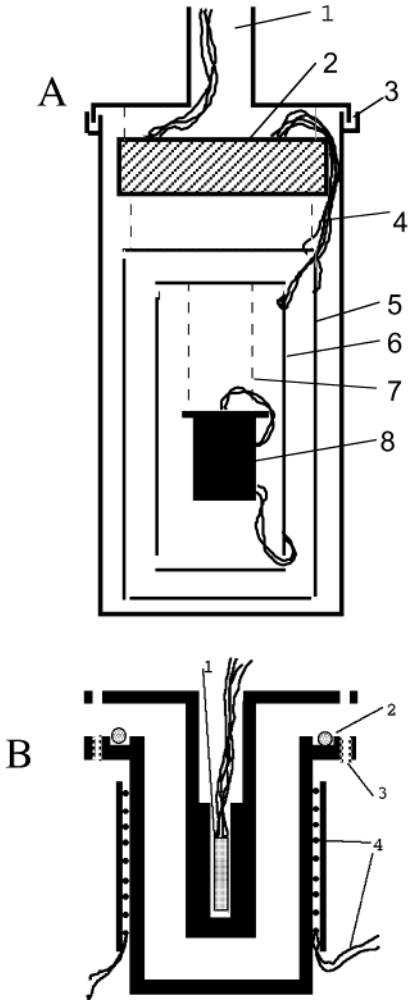

Figure 1. (A) Cross section of the cryostat: 1, pipe for evacuation; 2, thermal block made of copper; 3, seal with Wood's metal; 4, thin wires of heater, thermometer, and thermocouples; 5, outer adiabatic sheld; 6, inner adiabatic shield; 7, thin nylon thread; 8, cell. (B) Cross section of the cell: 1, themometer; 2, O-ring made of indium; 3, screw to fix the lid containing the thermometer; 4, heater for input of Joule heat.

ments of heat capacity C_p with an adiabatic calorimeter. To test the relationship between the dynamical heterogeneity and thermodynamic behavior, we also performed dielectric measurements on the same solutions.

Experiment Section

Materials. Polystyrene (PS) was prepared by anionic polymerization in benzene by using *sec*-butyllithium as the initiator. The weight-average molecular weight M_w and the polydispersity M_w/M_n were determined to be 7.5×10^5 and 1.10, respectively, by using gel permeation chromatograph (GPC). Toluene was used for PS solutions with PS concentration above 30 wt %, but for measurements of the solvent and 20 wt % solution we used a mixed solvent composed of toluene and xylene to avoid crystallization of the solvent. Specifically, mixtures of toluene/*o*-xylene/*m*-xylene 90/5/5 and 92/4/4 (by weight) were used for measurements of the solvent and 20 wt % PS solution, respectively. Toluene with purity higher than 99% and xylenes with ca. 98% purity were obtained from Wako Pure Chemical Industries (Tokyo, Japan) and used without further purification.

Method. The cross-sectional view of the calorimeter is shown in Figure 1a. The whole cryostat is immersed in liquid nitrogen irrespective of the temperature of measurement of C_p. Inside of the cryostat is kept high vacuum of about 10^{-4} Pa.

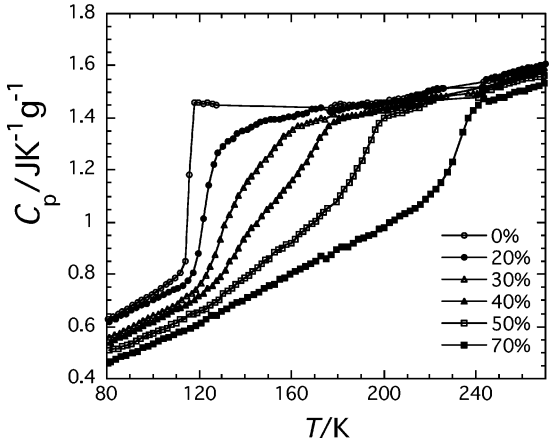

Figure 2. Specific heat capacities of toluene/xylene (90/10) and PS/toluene solutions.

The cell is surrounded by two thermal shields made of thin copper plates. The temperature difference between the inner thermal shield and the cell is controlled within 0.002 K, which is detected by a series connection of six copper−constantan thermocouples. Temperature of the outer shield is kept about 2 K lower than the inner shield. The thermal block plays a role to prevent heat conduction from the outside of the calorimeter through wires needed for measurements. Despite those efforts, a very small amount of heat flows between the cell and the shield. This heat flow can be calibrated by measurement of temperature drift. The cell has a capacity of 32 cm^3 and is made of copper (Figure 1b). An iron−rhodium resistance thermometer calibrated by Oxford Laboratiry (Oxford, UK) is placed at the center of the lid of the cell. Heating wire (manganin wire covered with silk) is wound around the cell. The cell is sealed by an O-ring made of indium (3 mm diameter). Measurements of resistance of the thermometer for measurement of temperature were made with a thermometry ac bridge (Automatic System Lab., model F700A, Milton Key, UK). The heat supplied to the cell was calculated from the voltage and current measured with a multimeter (Keithley, model 2000) with the four-terminal method. All measurements and controls were performed automatically by a personal computer (NEC9801) equipped with the GPIB (IEEE-488) system. The accuracy of the calorimeter was calibrated by measurements of C_p on purified benzoic acid, which is one of standard materials of calorimetry.[34] Before measurement of C_p, the cell containing a sample of ca. 20 g was cooled from room temperature to 80 K at cooling rate of ca. −3 K/min by introducing helium into the cryostat. The temperature was raised 2 K in one measurement of C_p, and it took about 50 h for measurements from 80 to 300 K.

Dielectric measurements were made between 80 and 273 K with a capacitance bridge (General Ratio 1615A). The capacitance cell was of a parallel plate type for measurements on viscous liquids.[21]

Result and Discussion

Heat Capacity. The temperature dependences of C_p (in J g^{-1} K^{-1}) of the solvent (toluene/xylene (90/10) mixture) and PS/toluene solutions are shown in Figure 2.

We see that the solvent (denoted as 0%) exhibits sharp stepwise increase of C_p at 115 K. As mentioned above, toluene/xylene (90/10) was used to avoid crystallization of toluene. Pure toluene crystallized during the cooling at the rate of −3 K/min, and hence we could not measure the C_p of glassy toluene. In the range between 128 and 178 K, the data of toluene/xylene (90/10) were not obtained because of the crystallization which occurred since the average heating rate (ca. 0.07 K/min) was much slower than the cooling rate. Once crystallization

began, the temperature of the cell increased due to heat evolution, and adiabatic conditions became out of control. Yamamuro et al.[35] reported the temperature dependences of C_p of a mixture of toluene/benzene (90/10). The present C_p curve of toluene/xylene (90/10) is very close to that of toluene/benzene (90/10), indicating that the additives such as xylene and benzene do not affect much both T_g and the magnitude of C_p.

In Figure 2, we see that PS solutions exhibit a broader glass transition than the solvent. As mentioned in the Experimental Section, we used toluene/xylene (92/8) as the solvent of 20% solution, but for solutions above 30 wt % concentration, we used pure toluene as the solvent because the rate of crystallization of toluene in those solutions was slow above 30%. As seen typically for the 40% solution, the C_p curves around T_g are double-sigmoid. We also see that the broadness of the double-sigmoidal change of C_p depends on concentration. The sigmoidal changes in the high-temperature side is designated as "glass transition 1" and the low-temperature side as "glass transition 2". The corresponding glass transition temperatures T_{g1} and T_{g2}, respectively, shift systematically to high temperature with increasing PS concentration, and the double-sigmoidal behavior becomes less clear. The definition of T_{g1} and T_{g2} will be given later. Here it is noted that the data between 225 and 240 K for 30, 40, and 50 wt % solutions are omitted because of scattering of data. This is due to melting of small amount of poly(dimethylsiloxane) used as adhesive between the thermometer and the cell. The omission of the data in this narrow region does not affect the analyses of the present data since the dielectric data indicate there is no thermal anomaly of the PS/toluene system in this temperature range. This difficulty was avoided for measurements of 70% solution by using an adhesive having T_g higher than room temperature.

Configurational Heat Capacities of Solutions. Generally the heat capacity under constant pressure C_p of a supercooled liquid consists of the configurational heat capacity ΔC_p and the vibrational heat capacity $C_{p-\mathrm{vib}}$. The jump of heat capacity at T_g is due to a frozen-in process of the configuration and conformation of molecules.[36] Since our interest is in ΔC_p of PS/toluene solutions, we attempted to subtract $C_{p-\mathrm{vib}}$ from observed C_p as follows. In the glassy state where molecular rearrangements are completely frozen in, C_p is totally due to vibrations $C_{p-\mathrm{vib}}$ which can be further resolved into three parts: the heat capacity $C_{\mathrm{L-vib}}$ due to lattice vibrations, the heat capacity $C_{\mathrm{I-vib}}$ due to intramolecular vibrations, and $C_p - C_v$ the difference between C_p and the heat capacity under constant volume C_v. Since harmonic vibrations are independent of volume, the first two terms correspond to the heat capacity under constant volume ($C_{v-\mathrm{vib}}$). The small correction of $C_p - C_v$ is due to the unharmonicity of the vibrations. According to Nernst and Lindeman, $C_p - C_v$ is expressed by the form[37]

$$C_p - C_v = \alpha C_{v-\mathrm{vib}}{}^2 T \qquad (1)$$

where α is the constant, and we regard it as an adjustable parameter.

If the lattice vibration spectrum and the frequencies of the intravibration modes are known, $C_{\mathrm{L-vib}}$ and $C_{\mathrm{I-vib}}$ can be calculated by the sum of the Einstein functions.[38] Usually measurements of the lattice vibration spectra

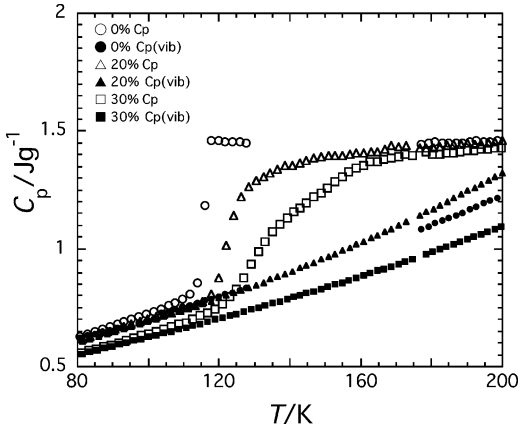

Figure 3. Observed C_p and C_p(vib) for toluene/xylene(90/10) (denoted as 0%), 20% PS solution, and 30 wt % PS solution.

are difficult, and the Debye approximation is frequently used.[39] In molecular crystals or glasses, there are three degrees of freedom of translational vibrations and three degrees of freedom of rotational vibration (libration) per one molecule. According to Yamamuro et al.,[35] the Debye temperature Θ_D of glassy toluene/benzene (90/10) is 100.7 K and the average frequency of the libration is 105.4 cm^{-1}. The number of modes of intramolecular vibrations is equal to $3N - 6$ per one molecule, where N is the number of atoms. For toluene ($N = 15$), Pitzer and Scott[40] reported the 38 frequencies of the normal modes. The remaining one mode is the rotational vibration of the methyl group and was estimated to be 28 cm^{-1}.[35] From these data we calculated $C_{v-\mathrm{vib}}$(Tol) in unit of J g^{-1} K^{-1} and was fitted to a polynomial:

$$C_{v-\mathrm{vib}} = A + BT + CT^2 + DT^3 + ET^4 \qquad (2)$$

where $A = 0.2367$, $B = 6.105347 \times 10^{-3}$, $C = -3.3017895 \times 10^{-5}$, $D = 1.530488 \times 10^{-7}$, and $E = 2.483286 \times 10^{-10}$. This equation agrees with $C_{v-\mathrm{vib}}$(Tol) within deviation of 0.5%. The parameter α of eq 1 was determined to be 0.001383 so that the observed and calculated heat capacities agree in the range from 80 to 90 K. Thus, calculated $C_{p-\mathrm{vib}}$ of toluene/xylene (90/10) is shown in Figure 3.

Wunderlich et al. measured C_p of glassy polystyrene and they estimated C_v based on the similar analyses mentioned above.[41−43] We have fitted the C_v (in J g^{-1} K^{-1}) data[41] to eq 2 with $A = 0.2966$, $B = -1.8222 \times 10^{-5}$, $C = 2.2374 \times 10^{-5}$, $D = 6.51190 \times 10^{-8}$, and $E = 7.63742 \times 10^{-11}$. The data reported by Wunderlich et al. and the calculated heat capacity with eq 2 agree well within deviation of 0.5%.

On the basis of thus-estimated $C_{v-\mathrm{vib}}$(PS) and $C_{v-\mathrm{vib}}$(Tol), we calculated $C_{v-\mathrm{vib}}$ of solutions. We assumed the additivity of the C_{vib}s of PS and the solvent:

$$C_{v-\mathrm{vib}}(\mathrm{PS/Tol}) = wC_{v-\mathrm{vib}}(\mathrm{PS}) + (1 - w)C_{v-\mathrm{vib}}(\mathrm{Tol}) \qquad (3)$$

where w is the weight fraction of PS. Then we determined α of eq 1 so that observed C_p agrees with the calculated $C_p = C_{v-\mathrm{vib}}(\mathrm{PS/Tol}) + C_p - C_v$ in the range from 80 to 90 K. The results are shown in Figures 3 and 4. Interestingly, ΔC_p of 70% solution starts to increase at about 120 K, which cannot be clearly recognized before estimation of $C_{p-\mathrm{vib}}$.

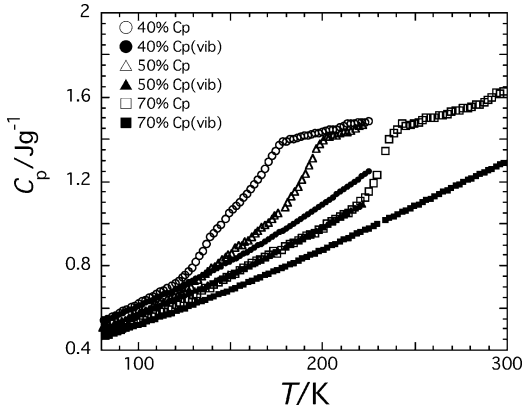

Figure 4. Observed C_p and C_p(vib) for PS solutions with concentrations of 40, 50, and 70 wt % PS solution.

Resolution of ΔC_p. We attempted to resolve ΔC_p into two steplike curves C_1 and C_2 assuming an empirical equation:

$$C_j \equiv \Delta C_j \frac{[1 - A_j(T - T_{gj})] \exp[B_j(T - T_{gj})]}{\exp[B_j(T - T_{gj})] + \exp[-B_j(T - T_{gj})]} \quad (4)$$

where j is either 1 or 2 and T_{gj}, B_j, and A_j are the fitting parameters. Here we define that the processes "1" and "2" are the high- and low-temperature processes, respectively. The glass transition temperature T_{gj} of each process is the inflection point of each sigmoidal curve. B_j is the parameter representing the broadness of the transition. The smaller the value of B_j, the broader the glass transition. A_j is the parameter representing the decrease of the configurational heat capacity with increasing temperature. We adopted a common value of A_j for processes 1 and 2. The parameters ΔC_j, B_j, A_j, and T_j are listed in Table 1, and the fitting curves are shown in Figure 5A−E. It is seen that the sum of the empirical curves C(calcd) = $C_1 + C_2$ agrees well with the experimental ΔC_p. Although the ΔC_p curves for 20% and 70% solutions appear to exhibit broad single glass

Table 1. Parameters of Eq 4

concn, wt %	process	ΔC_{pj}, J K^{-1}	$\Delta C_{pj}/w_j$, J g^{-1} K^{-1}	A_j	B_j	T_{gj}, K
20	1	0.080	0.40	0.0078	0.17	135
20	2	0.46	0.58	0.0078	0.25	122
30	1	0.15	0.50	0.0069	0.145	153
30	2	0.44	0.63	0.0069	0.092	130
40	1	0.19	0.48	0.0067	0.14	170
40	2	0.33	0.55	0.0067	0.061	140
50	1	0.33	0.66	0.0055	0.095	188
50	2	0.17	0.34	0.0055	0.043	143
70	1	0.36	0.51	0.0045	0.11	230
70	2	0.13	0.43	0.0042	0.025	145

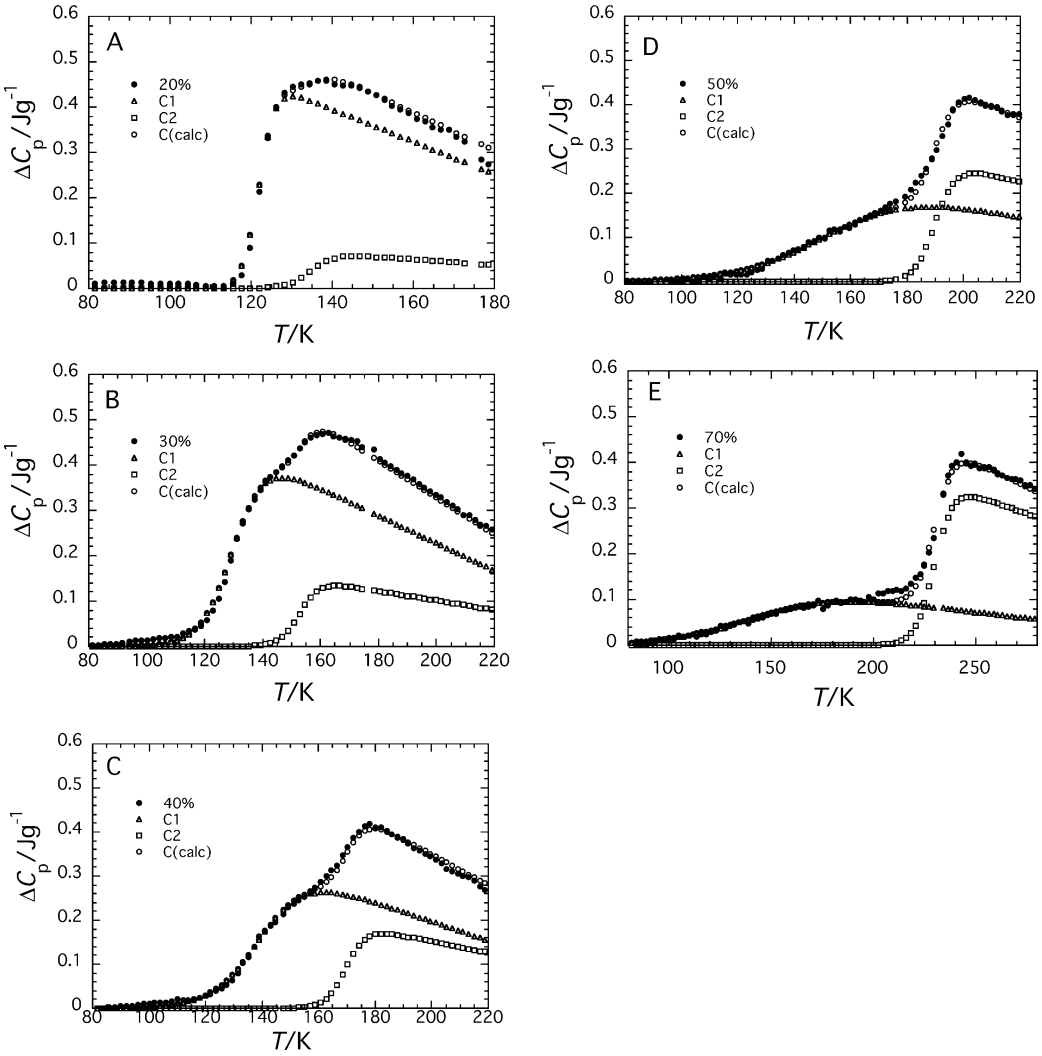

Figure 5. Configurational heat capacity $\Delta C_p = C_p$(obs) − C_p(vib) of PS solutions and the heat capacities C_1, C_2, and C(calcd) = $C_1 + C_2$ calculated with eq 4. Concentrations of PS are (A) 20, (B) 30, (C) 40, (D) 50, and (E) 70 wt %.

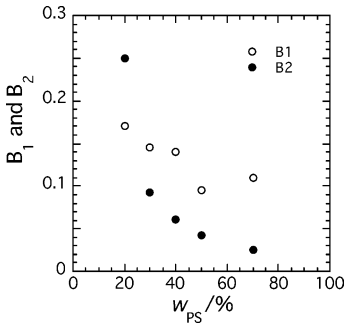

Figure 6. Dependences of B_1 and B_2 of eq 4 on the weight fraction w_{PS} of PS.

transitions, the present analyses indicate that these solutions can be resolved into the two glass transition processes.

So far it has been believed that polymers containing small amount of diluents (plasticizers) exhibit single glass transition accompanied by decrease of T_g. Figure 5E for 70% PS/toluene solution shows a broad glass transition due to toluene (T_{g2}) far below T_{g1}. Such a broad glass transition can be hardly detected by DSC and hence has been overlooked. Probably polymer/diluent systems generally exhibit such the double glass transition phenomenon even at low content of diluents.

In Table 1, it is seen that the ΔC_1 and T_{g1} increase monotonically with PS concentration, and hence process 1 is due to PS and process 2 is due to toluene as will be discussed in more detail in the next section. However, these parameters are not linear against PS concentration. Thus, resolved configurational heat capacities divided by weight fraction C_1/w_1 and C_2/w_2 correspond thermodynamically to the partial specific configurational heat capacities:

$$\Delta C_p = \left(\frac{\partial \Delta C_p}{\partial w_1}\right)_{w_2} w_1 + \left(\frac{\partial \Delta C_p}{\partial w_2}\right)_{w_1} w_2 = C_1 + C_2 \quad (5)$$

where w_1 and w_2 are the weight fraction of the components. Thus, C_1 and C_2 include the contributions of interactions between the components 1 and 2. This is the reason for the nonlinear dependences of the parameters.

Figure 6 shows the composition dependence of the parameters B_1 and B_2 which represent the broadness of the jumps of C_1 and C_2, respectively. Here it is reminded that the smaller the value of B, the broader the transition. It is seen that the broadness of the low-temperature process (process 2) increases steeply with increase of the PS content. On the other hand, the broadness of the high-temperature process does not change much and exhibits a minimum around $w_{PS} =$ 60%.

Thermal and Dielectric Glass Transition Temperatures. Representative temperature dependence curves of the dielectric loss ϵ'' for 30% solution are shown in Figure 7. The ϵ'' curves at 1 kHz of 20%, 30%, 40%, and 50% PS/toluene solutions are compared in Figure 8. According to Kauzmann, the calorimetric T_g corresponds to the temperature at which the dielectric relaxation frequency f_m becomes 0.001−0.0001 Hz.[30] We call this temperature the "dielectric T_g". Since the time scale τ of the present C_p measurements was about 1500 s, we define the dielectric T_g to be the temperature at which f_m ($=1/2\pi\tau$) becomes 0.0001 Hz.

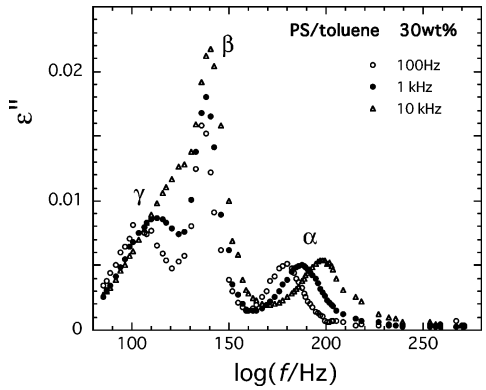

Figure 7. Temperature dependence of dielectric loss factor ϵ'' of 30 wt % solution of PS in toluene.

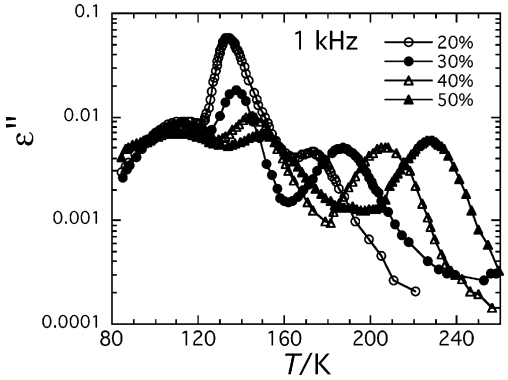

Figure 8. Comparison of ϵ'' curves of PS/toluene solutions with 20−50 wt % concentrations.

As reported previously, three loss peaks are seen for all solutions and are termed α, β, and γ in the order of decreasing temperature. Assignment of these peaks was reported previously. The α and β peaks are due to the primary (glass transition) processes arising from segmental motions of PS and rotation of the toluene molecules, respectively. As mentioned in the introductory section, the α and β peaks occur as the result of dynamical heterogeneity. The γ peak is the secondary relaxation of PS and toluene in the glassy state.[21] Floudas et al. studied dynamics in PS/toluene concentrated solutions by using depolarized Rayleigh scattering and dielectric spectroscopy. They also assigned the α and β processes to motions of PS and toluene, respectively.[31]

The Arrhenius plots for the loss maximum frequency f_m for the α and β processes are shown in parts A and B of Figure 9, respectively. In these figures we also plotted the data reported previously in refs 21 and 28. We extrapolated the Arrhenius plot for the α process to low-frequency side based on the Vogel−Fulcher equation[44,45] with parameters reported previously[21] and determined T_α. T_α of 70% solution was estimated from the dielectric data of 65 and 76 wt % solutions.

We determined T_β by linear extrapolation of the Arrhenius plots since the slope is high and the way of extrapolation does not cause much error in determination of T_β. It was observed that the intensity of the β process in solutions above 60% concentration became low. To enhance the β process, Yoshizaki et al.[28] used a mixed solvent composed of 95% of toluene and 5 wt % of *p*-chlorotoluene. In Figure 9B, we used those data only for the plots of 60 and 70 wt % solutions. Thus, determined T_α and T_β are compared with T_{g1} and T_{g2}

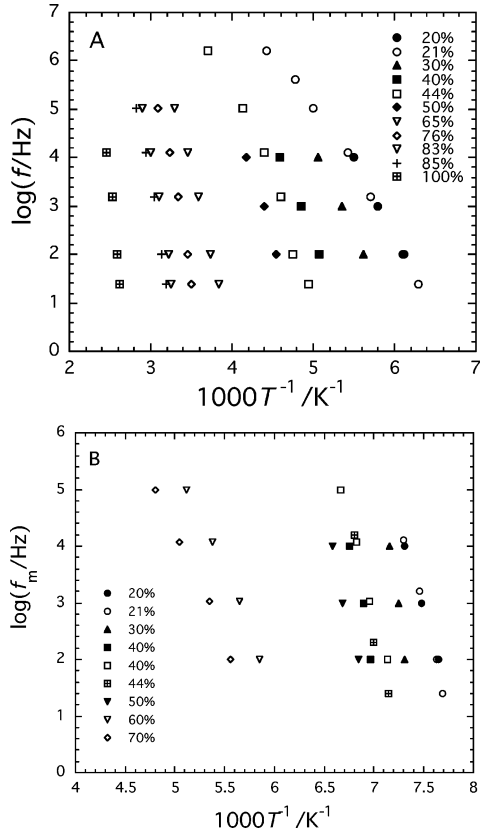

Figure 9. Arrhenius plots for the α process (A) and the β process (B). Closed keys indicate the present data, and open keys indicate the data reported in refs 21 and 28.

Table 2. Calorimetric and Dielectric Glass Transition Temperatures of the PS/Toluene System

w_{PS}	T_{g1}	T_α	T_{g2}	T_β
20	135	133	122	120
30	153	147	130	127
40	170	167	140	130
50	188	189	143	139
70	230	243	145	143

in Table 2. It is seen that T_{g1} and T_{g2} agree well with T_α and T_β, respectively. We conclude that the glass transitions 1 and 2 of PS/toluene solutions can be assigned to the freezing-in processes of motions of PS and toluene, respectively.

Lodge and McLeish proposed that the main origin of dynamical heterogeneity in polymer blends is due to effects of self-concentration.[19] They consider that local concentration of one component is always higher than average concentration due to the chain connectivity. There is no chain connectivity in diluent molecules, and hence there are no effects of self-concentration in small molecules. In fact, Savin et al. reported that mixtures of diluents do not exhibit broadening of glass transition.[33] The present PS/toluene system is intermediate of polymer blends and mixtures of diluents, but its behavior is close to polymer blends. It is expected that effects of self-concentration become predominant in the range of low PS concentration. But there is no positive evidence to support their model in the present data.

In Figure 6, we have seen that the broadness of T_{g1} changes moderately but that of T_{g2} increases steeply with the increase of PS content. This behavior is in agreement with the dielectric data of PS/toluene solutions reported by Yoshizaki et al., who reported that the half-width of the loss curve for the α process was independent of the concentration of PS, but that for the β process was nearly 2 times broader than that for α process.[28] The broadness of the glass transition for the β process reflects the distribution of the relaxation time which increased with PS concentration. Thus, the dependence of the broadness of the glass transition 2 on the PS content is consistent with the dielectric data.

The difference of the broadness of the C_p curves at T_{g1} and T_{g2} can be explained as follows. Below T_{g2} motions of the PS segments and toluene molecules are both frozen-in. Around T_{g2} the toluene molecules start to move, but the PS segments are still in the frozen-in state. In such the state the hindrance for motions of the toluene molecules depends on number of the neighboring PS segments surrounding toluene. If a toluene molecule is surrounded by the toluene molecules, it can move easily, but if surrounded by the PS segments, its motions are heavily damped. Therefore, the distribution of relaxation time is broad around T_{g2}. On the other hand, the PS segments start to move at T_{g1} in a situation that toluene molecules are moving fast. We expect that motions of toluene smear out the heterogeneity, and hence the jump of C_p at T_{g1} is relatively narrow.

Jump of Heat Capacity at T_g. The magnitude of the jump of heat capacity ΔC_p at T_g is one of unsolved issues. Roe and Tonelli[46] reported that the conformational heat capacities of various polymers calculated with the rotational isomeric state model are much lower than observed ΔC_p.[47] Thus, the configuration of molecules plays dominant contribution to ΔC_p of polymers. This is in harmony with the fact that toluene/xylene (90/10) having no isomeric states exhibits similar ΔC_p to PS.

In the temperature range between T_{g1} and T_{g2}, segmental motions of the PS chains are frozen-in, but motions of the toluene molecules are not frozen-in. In such a situation, the intermolecular interactions between PS and toluene are not frozen-in. Therefore, we expect that the jump of heat capacity at T_{g1} is mostly due to the conformational heat capacity. However, as is seen in Table 1, $\Delta C_1/w_1$ is slightly larger than ΔC_p (= 0.29 J K^{-1} g^{-1}) of pure PS.

Conclusion

The heat capacity C_p of concentrated toluene solutions of polystyrene (PS) has been measured by using an adiabatic calorimeter. The C_p vs temperature T curves of PS/toluene solutions are double-sigmoidal. The configurational heat capacity ΔC_p can be resolved into two sigmoidal curves C_1 and C_2. The glass transition temperatures T_{g1} and T_{g2} ($T_{g1} > T_{g2}$) corresponding to the two sigmoids agree with the dielectric glass transition temperatures T_α and T_β, respectively, which are defined as the temperatures at which the dielectric relaxation frequencies for the α and β processes of the PS/toluene system become 10^{-4} Hz. Since the α and β processes can be assigned to segmental motions of PS and rotation of the toluene molecules, respectively, T_{g1} and T_{g2} are assigned to the temperatures at which motions of PS and toluene are frozen in, respectively. We conclude that dynamically heterogeneous systems composed of mobile and less mobile components exhibit glass transition at different temperatures. The jump of the heat capacities ΔC_p at T_g for PS is much larger than the conformational heat capacity calculated on the basis of the rotational isomeric states. The broadness of the glass transition

for the each component depends on the composition of PS/toluene. The broadness of the glass transition due to toluene increases steeply with increasing PS content. The present study will be extended to miscible polymer blends such as polyisoprene/poly(vinylethylene).

References and Notes

(1) Runt, J. R. In *Dielectric Spectroscopy of Polymeric Materials*; Runt, J. P., Fitzgerald, Eds.; American Chemical Society: Washington, DC, 1997; Chapter 10, pp 283−302.
(2) Roland, C. M.; Ngai, K. L. *Macromolecules* **1992**, *25*, 363.
(3) Algeria, A.; Colmenero, J.; Ngai, K. L.; Roland, C. M. *Macromolecules* **1994**, *27*, 4486.
(4) Alvarez, F.; Alegria, A.; Colmenero, J. *Macromolecules* **1997**, *30*, 597.
(5) Arbe, A.; Alegria, A.; Colmenero, J.; Hoffman, S.; Willner, L.; Richter, D. *Macromolecules* **1999**, *32*, 7572.
(6) Hayakawa, T.; Adachi, K. *Macromolecules* **2000**, *33*, 6834.
(7) Urakawa, O.; Fuse, Y.; Hori, H.; Qui, T.; Yano, O. *Polymer* **2001**, *42*, 765.
(8) Zhang, S. H.; Jin, X.; Painter, P. C.; Runt, J. *Macromolecules* **2003**, *36*, 5710.
(9) Jin, X.; Zhang, S. H.; Runt, J. *Macromolecules* **2003**, *36*, 8033.
(10) Miller, J. B.; McGrath, K. J.; Roland, C. M.; Trask, C. A.; Garroway, A. N. *Macromolecules* **1990**, *23*, 4543.
(11) Roland, C. M.; Ngai, K. L. *Macromolecules* **1991**, *24*, 2261.
(12) Rizos, A.; Fytas, G.; Alig, I, Kremer, F.; Pakula, T. *Polymer* **1993**, *34*, 2263.
(13) White, J. L.; Mirau, P. *Macromolecules* **1993**, *26*, 3049.
(14) Chung, G.-C.; Kornfield, J. A.; Smith, S. D. *Macromolecules* **1994**, *27*, 964.
(15) Gisser, D. J.; Ediger, M. D. *Macromolecules* **1994**, *27*, 5729.
(16) Li, S.; Rice, D. M.; Karasz, F. E. *Macromolecules* **1992**, *25*, 1284.
(17) Katana, G.; Fischer, E. W.; Hack, Th.; Abetz, V.; Kremer, F. *Macromolecules* **1995**, *28*, 2714.
(18) Zetsche, A.; Fischer, E. W. *Acta Polym.* **1994**, *45*, 168.
(19) Lodge, T. P.; McLeish, T. C. B. *Macromolecules* **2000**, *33*, 5278.
(20) Tomlin, D. W.; Roland, C. M. *Macromolecules* **1992**, *25*, 2994.
(21) Adachi, K.; Fujihara, I.; Ishida, Y. *J. Polym. Sci., Polym. Phys. Ed.* **1975**, *13*, 2155.
(22) Adachi, K.; Ishida, Y. *J. Polym. Sci., Polym. Phys. Ed.* **1976**, *14*, 2219.
(23) Adachi, K.; Hattori, M.; Ishida, Y. *J. Polym. Sci., Polym. Phys. Ed.* **1977**, *15*, 693.
(24) Adachi, K.; Ishida, Y. *Polym. J.* **1979**, *11*, 233.
(25) Adachi, K.; Kotaka, T. *Polym. J.* **1981**, *13*, 687.
(26) Yada, M.; Nakazawa, M.; Urakawa, O.; Morishima, Y.; Adachi, K. *Macromolecules* **2000**, *33*, 3368.
(27) Nakazawa, M.; Urakawa, O.; Adachi, K. *Macromolecules* **2000**, *33*, 7898.
(28) Yoshizaki, K; Urakawa, O.; Adachi, K. *Macromolecules* **2003**, *36*, 2349.
(29) Hori, H.; Urakawa, O.; Adachi, K. *Polym. J.* **2003**, *35*, 721.
(30) Kauzmann, W. *Chem. Rev.* **1948**, *43*, 219.
(31) Floudas, G.; Steffan, W.; Fischer, E, W.; Browm, W. *J. Chem. Phys.* **1993**, *99*, 695.
(32) Ceccorulli, G.; Pizzori, M.; Scandola, M. *Polymer* **1987**, *28*, 2077.
(33) Savin, D. A.; Larson, A. M.; Lodge, T. P. *J. Polym. Sci., Part B: Polym. Phys. Ed.* **2004**, *42*, 1155.
(34) MxCullough J. P.; Scott, D. W. *Calorimetry of Non-reacting Systems*; Butterworth: London, 1968.
(35) Yamamuro, O.; Tsukusi, I.; Lindqvist, A.; Takahara, S.; Ishikawa, M.; Matsuo, T. *J. Phys. Chem. B* **1998**, *102*, 1605.
(36) Shen, M. C.; Eisenberg, A. *Prog. Solid State Chem.* **1967**, *3*, 407.
(37) Nersnst, W.; Lindemann, F. *Electrochemistry* **1911**, *17*, 817.
(38) Einstein, A. *Ann. Phys. (Leipzig)* **1907**, *22*, 180.
(39) Debye, P. *Ann. Phys. (Leipzig)* **1912**, *789*, 180.
(40) Pitzer, K.; Scott, B. *J. Am. Chem. Soc.* **1943**, *65*, 803.
(41) Kirkpatrick, D. E.; Judovits, L.; Wunderlich, B. *J. Polym. Sci., Polym. Phys. Ed.* **1986**, *24*, 45.
(42) Judovits, L. H.; Bopp, R. C.; Gaur, U.; Wunderlich, B. *J. Polym. Sci., Polym. Phys. Ed.* **1986**, *24*, 2725.
(43) Gaur, U.; Wunderlich, B. *J. Phys. Chem.* **1982**, *11*, 313.
(44) Vogel, H. *Phys. Z.* **1921**, *22*, 645.
(45) Fulcher, G. A. *J. Am. Ceram. Soc.* **1925**, *8*, 339.
(46) Roe, R.-J.; Tonelli, A. E. *Macromolecules* **1978**, *11*, 114.
(47) Yoon, D. Y.; Sundararajan, P. R.; Flory, P. J. *Macromolecules* **1975**, *8*, 776.

MA048788J